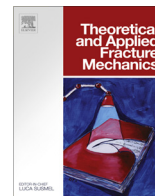




Contents lists available at ScienceDirect

Theoretical and Applied Fracture Mechanics

journal homepage: www.elsevier.com/locate/tafmec

Calculation of stress intensity factor for functionally graded cylinders with two radial cracks using the weight function method

Hassan Mirahmadi^a, Majid Azimi^b, Seyed Sajad Mirjavadi^{a,*}

^a School of Mechanical Engineering, College of Engineering, University of Tehran, Tehran, Iran

^b School of Mechanical Engineering, College of Engineering, Sharif University of Technology, Tehran, Iran

ARTICLE INFO

Article history:

Received 19 February 2016

Revised 1 June 2016

Accepted 14 June 2016

Available online xxx

Keywords:

Radial crack

Hollow cylinder

Stress intensity factor

Functionally graded material

Weight function

ABSTRACT

In this study, obtaining stress intensity factors (SIFs) for functionally graded cylinders with two internal radial cracks using the weight function method has been discussed. For this purpose, reference SIFs are calculated from the results of finite element analysis, using a modified domain of the J integral. Subsequently, SIFs have been calculated for different combinations of cylinder geometry, crack depth, and material gradation by implementing the weight function method and it is shown that the results are consistent with corresponding results obtained from finite element analysis. Moreover, the effects of variation in the elastic modulus ratio on SIFs have been investigated.

© 2016 Published by Elsevier Ltd.

1. Introduction

Functionally graded materials (FGMs) are compound materials in which mechanical properties vary continuously from one point to another or from surface to surface. Due to their desirable thermal and mechanical properties, FGMs can have various applications in industry, thus, they have received much attention from scientists and engineers of different fields [1].

The volume fraction of constituents in the FGMs changes continuously based on a specific function, and therefore, there will be no discontinuity in the mechanical properties. These materials can be used as a binder of two different layers to improve bond strength [2] and also eliminate delamination [3] and stress concentration [4,5]. Due to the advantages of FG materials compared to composites and homogenous materials, they are implemented in various areas such as space-type applications, electronics and magnetism [6].

Great efforts have been made to investigate fracture mechanics parameters in FGMs. Wei and Shih [7] studied several important concepts of interface fracture mechanics. Jin and Batra [8] presented the basic concepts of classical fracture mechanics in FGMs. Erdogan [4] investigated the singularity of stresses near the crack tip in nonhomogeneous materials. Kim and Paulino [6] studied SIFs

in FG materials using the modified crack closure integral (MCCI) method. Walters et al. [9] explored SIFs in FG plates under mode-I thermomechanical loading. Yildirim et al. [10] investigated fracture analysis of semi-elliptical surface cracks in FGM coatings subjected to thermomechanical loading. Zhang et al. [11] obtained properties of 3-dimensional cracks in FGMs. First, they calculated crack tip displacement using the boundary element method after which they calculated SIFs according to the relevant relations. Afsar and Anisuzzaman [1] studied thick-walled FG cylinders with two internal axial cracks and calculated SIFs using numerical methods. They considered the FG cylinder as some cylindrical layers of limited thickness in a way that properties are constant in each layer.

The weight function method was first introduced in [12,13]. This method has been used extensively for calculating SIFs in cracked structures and for arbitrary loading conditions. The weight function is independent of loading conditions but depends on crack geometry. If the weight function of a certain geometry is specified, integrating the multiplication of the weight function and stress along the crack length will yield the SIF [14]. Fett and Munz [15,16] extended weight function method for FG crack problems based on the theory of Bueckner [12] and superposition principle. Eshraghi and Soltani [17,18] have demonstrated the precision of the weight function method based on the theory of Bueckner in calculating the SIF of circumferential cracks in FG cylinders subjected to mechanical and thermal loads. Shi et al. [19] derived the basic weight function equations for two-dimensional FG

* Corresponding author.

E-mail addresses: h.mirahmadi@ut.ac.ir (H. Mirahmadi), nabatighanbari@yahoo.com (M. Azimi), s.mirjavadi@ut.ac.ir (S.S. Mirjavadi).

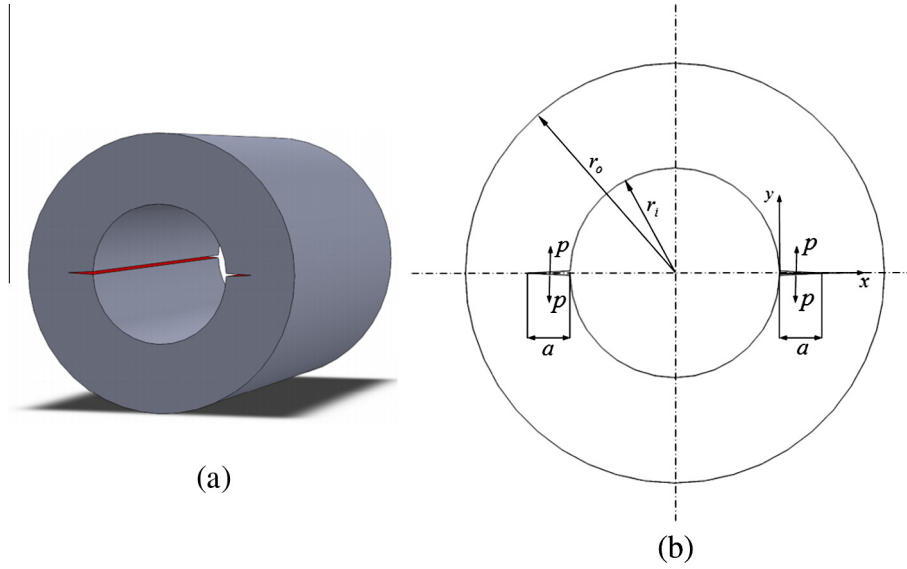


Fig. 1. A cylinder with two internal radial cracks.

$$M_2 = 21 + \frac{\pi}{\sqrt{2}} \left[-\frac{105}{2} Y_0 + 315 \frac{Y_1}{\left(\frac{a}{r_o - r_i}\right)} - 315 \frac{Y_2}{\left(\frac{a}{r_o - r_i}\right)^2} \right] \quad (5b)$$

$$M_3 = -\frac{64}{5} + \frac{\pi}{\sqrt{2}} \left[48 Y_0 - 264 \frac{Y_1}{\left(\frac{a}{r_o - r_i}\right)} + 252 \frac{Y_2}{\left(\frac{a}{r_o - r_i}\right)^2} \right] \quad (5c)$$

in which $Y_i = K_i / (A_i \sqrt{\pi a})$ ($i = 1, 2, 3$) are dimensionless reference SIFs.

3. Modified J integral calculation

The energy release rate in FG materials under the conditions of mode I, similar to Fig. 2, is calculated by Eq. (6) [14]:

$$J = \lim_{\Gamma_\varepsilon \rightarrow 0} \left\{ \int_{\Gamma_\varepsilon} \{ W n_1 - \sigma_{ij} n_j u_{i,1} \} ds \right\} \quad (i, j = 1, 2) \quad (6)$$

where Γ_ε implies curve around the crack tip which is elongated from lower crack surface to the upper one. Moreover, x_1 and x_2 imply the principal directions, S denotes the curve length, W is

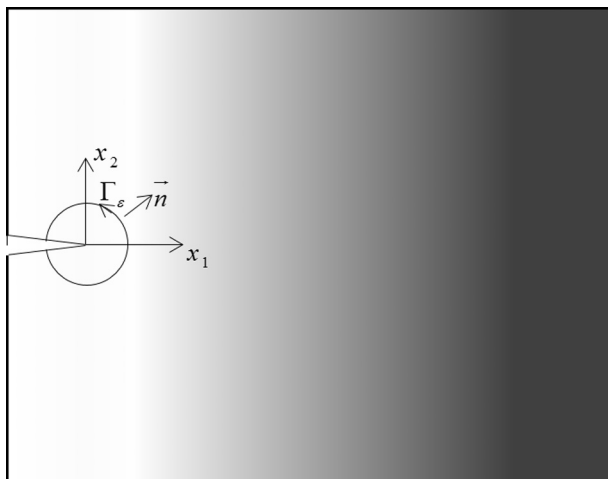


Fig. 2. A crack in a functionally graded material.

the energy density function of mechanical strain, n_i ($i = 1, 2$) is the unit outward normal vector, σ_{ij} and u_i ($i, j = 1, 2$) denote the stress and displacement components respectively, and $(\cdot)_{,j} \equiv \frac{\partial(\cdot)}{\partial x_j}$.

Based on Eq. (6), Dag [28] represented the energy release rate in the form of domain integral by Eq. (7):

$$J = \lim_{\Gamma_\varepsilon \rightarrow 0} \left\{ \int_{\Gamma_\varepsilon} \{ W n_1 - \sigma_{ij} n_j u_{i,1} \} ds \right\} \\ = \iint_{\Omega} \{ \sigma_{ij} u_{i,1} - W \delta_{1j} \} q_j d\Omega - \iint_{\Omega} (W_{,1})_{\text{expl}} q d\Omega \quad (i, j = 1, 2) \quad (7)$$

in which δ_{ij} ($i, j = 1, 2$) is the Kronecker delta function, q is the vector representing a smooth function that changes from unity at the crack front to zero at the boundary of the domain of integration, $(W_{,1})_{\text{expl}}$ is the explicit derivative of the strain energy which is defined as:

$$(W_{,1})_{\text{expl}} = \frac{\partial W}{\partial E} \frac{\partial E}{\partial x_1} \quad (8)$$

and Ω is domain of integration.

Dag [28] also recommended the following function for q :

$$q(x_1, x_2) = 1 - \frac{\sqrt{x_1^2 + x_2^2}}{R} \quad (9)$$

where R is the radius of the domain of integration (centered at the crack tip) and x_1 and x_2 are the crack tip in-plane coordinates, as shown in Fig. 3.

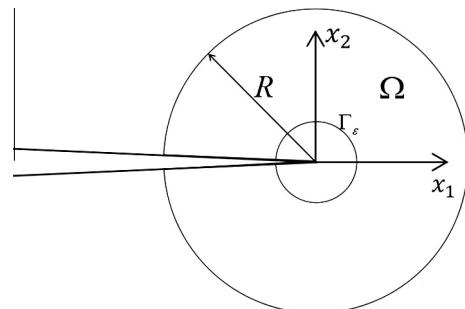


Fig. 3. Domain of integration for energy release rate calculation.

When the J integral is obtained, the mode-I SIF can be derived using the material properties at the crack tip location (Eq. (10)):

$$K_I = \sqrt{J E_{tip}^*} \quad (10)$$

where $E_{tip}^* = E_{tip}$ for plane stress and $E_{tip}^* = E_{tip}/(1 - \nu_{tip}^2)$ for plane strain conditions. E_{tip} is the elastic modulus and ν_{tip} is Poisson's ratio of the material at the crack tip location [17].

4. FE modeling and validation

4.1. Validation of modified J integral calculation

Two numerical examples are presented to prove the accuracy of proposed method. In both examples, it is assumed that young's modulus, varies with the variation of coordinate system, while Poisson's ratio is constant. Delale et al. [29] shown that the effect of Poisson's ratio variation in comparison with young's modulus is negligible. Fig. 4a shows a plane with the length of $L = 8$ units and width of $B = 1$ unit with an edge crack with the length of a . Loading conditions are $\sigma_{22}(x_1, \pm 4) = \pm 1.0$ for uniform tension and $\sigma_{22} = \pm(-2x_1 + 1)$ for bending (shown in Fig. 4b). Boundary conditions in $a \leq x_1 \leq 1$ region and on line $x_2 = 0$ is: $u_2 = 0$. Moreover, for the right node of the region, $u_1 = 0$. Young's modulus variation is also exponentially assumed as Eq. (11):

$$E(x_1) = E_1 e^{\lambda x_1} \quad (0 \leq x_1 \leq 1) \quad (11)$$

In this equation, $\lambda = \log(E_2/E_1)$ and $E(0) = E_1 = 1.0$; so $E(1) = E_2$. For finite element analysis, Poisson's ratio of $\nu = 0.3$, $E_2/E_1 = (0.1, 0.2, 1, 5, 10)$, $a/B = (0.2, 0.3, 0.4, 0.5, 0.6)$, and plane strain conditions are assumed. Using the method proposed in Tables 1 and 2, results of finite element analysis are compared to the results reported by Erdogan and Wu [30] and Kim and Paulino [31].

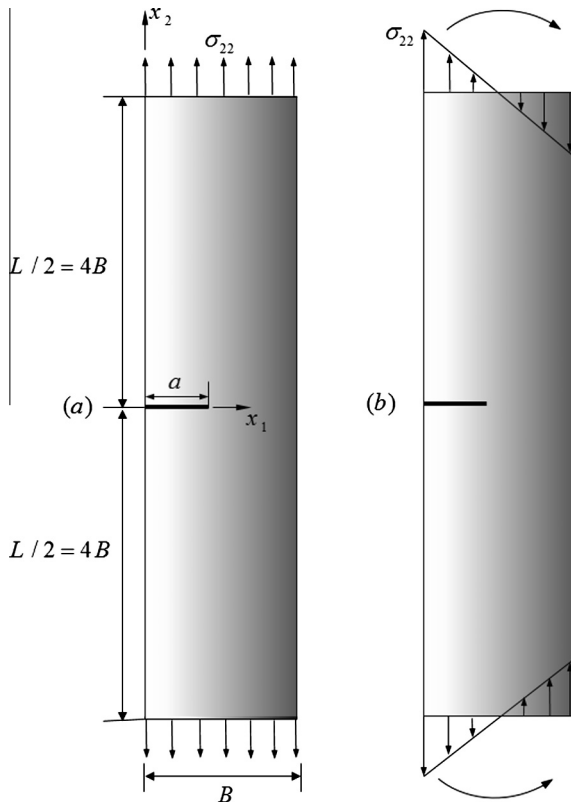


Fig. 4. Configurations for edge cracked plate: (a) tension loading; (b) bending loading.

Table 1

Normalized stress intensity factors for edge cracked plate under tension.

	E2/E1	a/B				
		0.2	0.3	0.4	0.5	0.6
Erdogan and Wu [30]	0.1	1.904	1.885	1.977	2.215	2.717
	0.2	1.595	1.612	1.721	1.953	2.403
	1	–	–	–	–	–
	5	0.687	0.777	0.923	1.151	1.559
	10	0.564	0.658	0.804	1.035	1.428
Kim and Paulino [31]	0.1	1.888	1.864	1.943	2.145	2.553
	0.2	1.588	1.601	1.706	1.925	2.341
	1	1.055	1.122	1.26	1.496	1.913
	5	0.687	0.778	0.924	1.158	1.561
	10	0.565	0.659	0.804	1.035	1.429
Present work	0.1	1.879	1.850	1.922	2.122	2.545
	0.2	1.582	1.592	1.693	1.902	2.322
	1	1.055	1.123	1.260	1.493	1.913
	5	0.691	0.781	0.931	1.168	1.575
	10	0.569	0.663	0.814	1.048	1.446

Table 2

Normalized stress intensity factors for edge cracked plate under bending.

	E2/E1	a/B				
		0.2	0.3	0.4	0.5	0.6
Erdogan and Wu [30]	0.1	1.296	1.858	2.569	3.570	5.188
	0.2	1.395	1.839	2.443	3.326	4.761
	1	–	–	–	–	–
	5	1.131	1.369	1.748	2.365	3.445
	10	1.001	1.229	1.588	2.176	3.212
Kim and Paulino [31]	0.1	1.284	1.846	2.554	3.496	4.962
	0.2	1.39	1.831	2.431	3.292	4.669
	1	1.358	1.658	2.11	2.822	4.03
	5	1.132	1.37	1.749	2.366	3.448
	10	1.003	1.228	1.588	2.175	3.212
Present work	0.1	1.284	1.830	2.518	3.456	4.950
	0.2	1.386	1.819	2.413	3.253	4.635
	1	1.367	1.659	2.111	2.817	4.033
	5	1.138	1.375	1.764	2.387	3.479
	10	1.009	1.236	1.608	2.205	3.254

Considering the results of Erdogan and Wu [30] as the reference shows that the result of the present study is consistent with J integral method proposed by Kim and Paulino [31].

4.2. Validation of present FE model

In order to decrease the computational costs of simulating the cylinder with two internal radial cracks (shown in Fig. 1), just one fourth of the cylinder is modeled because of the symmetry along its horizontal and vertical axes. The FE model of the cylinder is shown in Fig. 5. Finite elements modeling is conducted by ABAQUS Standard software [32]. ABAQUS user subroutines USDFLD and UFIELD are written for applying elastic modulus gradation in FG cylinder. Moreover, an ABAQUS Python script is written for automating the generation of finite element models with variations in their effective parameters, which are internal to external radius, crack depth to cylinder thickness, and elastic modulus ratios. The size of elements around the crack tip is 1% of the crack depth in all FE models. Since a very fine mesh is used near the crack tip (shown in Fig. 5), SIFs were not affected by the size of elements in that region; therefore convergent finite elements results are obtained. 8-node biquadratic plane strain quadrilateral, reduced integration elements (CPE8R) are used for meshing the models.

In post-processing step, the nodal displacements obtained by finite element analysis is used to calculate modified domain of the J contour integral for six contours around the crack tip

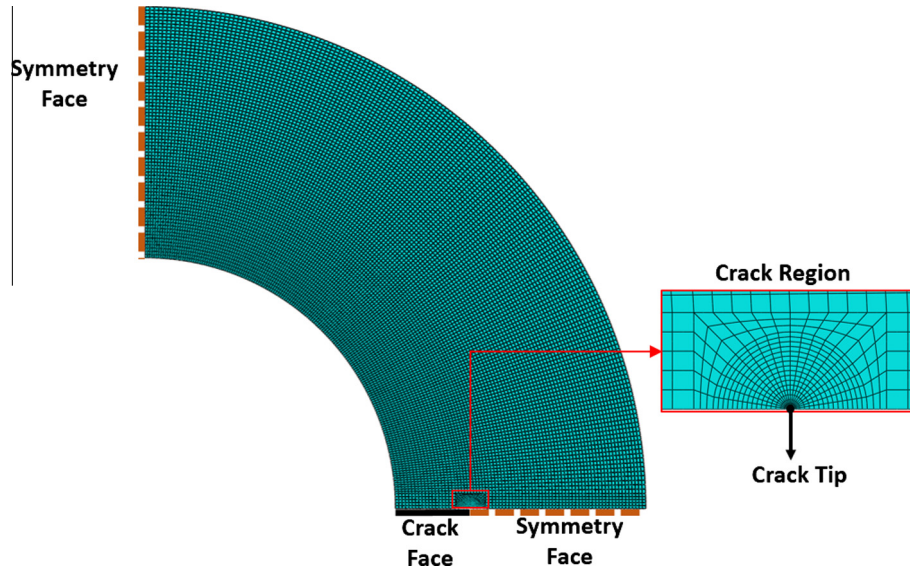


Fig. 5. Finite element mesh of one fourth cylinder (left), and close up of the mesh near the crack tip (right).

(discussed in Section 3). J integral value of the nearest contour to the crack tip is ignored and the average of the remaining five is considered as the J integral to obtain SIFs based on Eq. (10).

In order to validate the FE model, homogenous cylinders with two internal radial cracks are simulated the two following cases:

Case (A) $r_i/r_o = 2.0$ and pressure on crack plane:

$$p(x) = A[x/(r_o - r_i)]^2 \quad (0 \leq x \leq a).$$

Case (B) $r_i/r_o = 2.5$ and pressure on crack plane:

$$p(x) = A[x/(r_o - r_i)]^4 \quad (0 \leq x \leq a).$$

Assuming plane strain conditions in the analysis, normalized SIFs is calculated by Eq. (12)

$$K_I^N = K_I / (A\sqrt{\pi a}) \quad (12)$$

The results of this analysis have been compared with extracted results from [22] presented in Table 3, and it can be seen that the results are in good consistency.

4.3. Weight functions for FG cylinders

Using the FE model and modified form of J integral, reference SIFs are calculated by Eq. (4). Subsequently, weight functions for FG cylinder can be determined using Eq. (5).

Elastic modulus of FG cylinder varies along its thickness according to the following exponential function:

$$E(r) = E_i \exp(\lambda(r - r_i)/(r_o - r_i)) \quad (r_i \leq r \leq r_o) \quad (13)$$

where E_i and r represent elastic modulus at $r = r_i$ and distance of an arbitrary point from center of the cylinder, respectively. In the present work, Poisson's ratio is considered to be constant and equal to

0.3. Parameter λ can be expressed by the ratio of elasticity modulus in internal and external surfaces denoted by E_i and E_o respectively:

$$\lambda = \ln \frac{E_o}{E_i} = \ln \gamma \quad (14)$$

where $\gamma = E_o/E_i$ is the elastic modulus ratio of FG cylinder.

In present FE models, the ratios of internal to external radius and crack depth to thickness vary from 0.1 to 0.8 with the step value of 0.1. In addition, various values are considered for the elastic modulus ratio of the FG cylinder ($\gamma = 0.1, 0.2, 0.5, 1, 5, 10$).

In all generated models, radius and the elastic modulus at the internal surface are considered to be constant and equal to 50 mm and 100 GPa respectively.

In addition to three reference load cases (Eq. (4)), FE solution is performed for cubic and periodic loadings (similar to the procedure followed in [17]). The SIFs related to these two load cases are used for investigating the weight function method accuracy in stress intensity estimation and are not involved in calculation of weight function. Thus, five load cases are applied on surfaces of two radial cracks that are defined as:

$$\text{Load Case no. 1 : uniform distribution } \sigma(x) = \sigma_0 \quad (15a)$$

$$\text{Load Case no. 2 : linear distribution } \sigma(x) = \sigma_0 \left(\frac{x}{r_o - r_i} \right) \quad (15b)$$

$$\text{Load Case no. 3 : quadratic distribution } \sigma(x) = \sigma_0 \left(\frac{x}{r_o - r_i} \right)^2 \quad (15c)$$

Table 4

FE modeling matrix for weight function determination and comparison.

Variable	Range	Number of variations	Total number of FE runs
Cylinder geometry ($\alpha = r_i/r_o$)	0.1–0.8 (increment = 0.1)	8	–
Crack geometry ($\beta = a/t$)	0.1–0.8 (increment = 0.1)	8	–
Elastic modulus ratio ($\gamma = E_o/E_i$)	0.1, 0.2, 0.5, 1, 5, 10	7	–
Reference load cases (15a, 15b, 15c)	Uniform, linear, quadratic	3	1344 (for weight function development)
Additional load cases (15d, 15e)	Cubic, periodic	2	896 (for result comparison)

Table 3

Comparison of normalized SIFs for cylinders with two internal radial cracks.

$a/(r_o - r_i)$	Case(A)		Case(B)	
	Ref. [22]	Present FE	Ref. [22]	Present FE
0.2	2.203E–02	2.201E–02	6.320E–04	6.307E–04
0.4	9.990E–02	9.990E–02	1.089E–02	1.086E–02
0.6	2.633E–01	2.634E–01	6.085E–02	6.078E–02
0.8	5.806E–01	5.792E–01	2.265E–01	2.266E–01

Table 5Normalized SIFs for various FG cylinder geometries with $\gamma = 10$ obtained by the weight function method and direct FE analysis.

α	Load case	Method	$\beta = 0.1$	$\beta = 0.2$	$\beta = 0.3$	$\beta = 0.4$	$\beta = 0.5$	$\beta = 0.6$	$\beta = 0.7$	$\beta = 0.8$
0.2	1	FE	0.9358	0.9256	0.9756	1.0772	1.2409	1.4902	1.8670	2.4552
	1	WE	0.9358	0.9256	0.9755	1.0772	1.2408	1.4901	1.8667	2.4546
	2	FE	0.0610	0.1214	0.1881	0.2670	0.3665	0.5004	0.6926	0.9916
	2	WE	0.0610	0.1214	0.1881	0.2670	0.3665	0.5004	0.6924	0.9913
	3	FE	0.0048	0.0193	0.0445	0.0828	0.1388	0.2208	0.3447	0.5447
	3	WE	0.0048	0.0193	0.0445	0.0829	0.1388	0.2208	0.3446	0.5445
	4	FE	0.9354	0.9223	0.9642	1.0493	1.1833	1.3823	1.6748	2.1169
	4	WE	0.9354	0.9223	0.9642	1.0492	1.1831	1.3820	1.6743	2.1162
	5	FE	0.4266	0.4168	0.4539	0.5297	0.6515	0.8360	1.1123	1.5361
	5	WE	0.4263	0.4165	0.4535	0.5293	0.6511	0.8356	1.1119	1.5357
0.4	1	FE	1.0136	1.0270	1.1055	1.2470	1.4674	1.7975	2.2850	3.0048
	1	WE	1.0135	1.0270	1.1055	1.2469	1.4673	1.7973	2.2847	3.0042
	2	FE	0.0640	0.1294	0.2033	0.2930	0.4087	0.5669	0.7947	1.1403
	2	WE	0.0640	0.1294	0.2034	0.2930	0.4087	0.5669	0.7945	1.1400
	3	FE	0.0050	0.0202	0.0471	0.0886	0.1504	0.2422	0.3821	0.6056
	3	WE	0.0050	0.0202	0.0471	0.0886	0.1504	0.2422	0.3821	0.6054
	4	FE	1.0131	1.0236	1.0937	1.2176	1.4060	1.6813	2.0763	2.6365
	4	WE	1.0130	1.0236	1.0936	1.2175	1.4058	1.6810	2.0758	2.6357
	5	FE	0.4854	0.4932	0.5520	0.6590	0.8262	1.0765	1.4441	1.9780
	5	WE	0.4850	0.4928	0.5516	0.6586	0.8258	1.0760	1.4436	1.9776
0.6	1	FE	1.0578	1.1014	1.2193	1.4197	1.7326	2.2116	2.9380	4.0092
	1	WE	1.0577	1.1014	1.2192	1.4196	1.7324	2.2113	2.9376	4.0086
	2	FE	0.0658	0.1352	0.2166	0.3195	0.4583	0.6573	0.9563	1.4167
	2	WE	0.0658	0.1352	0.2167	0.3195	0.4583	0.6572	0.9561	1.4164
	3	FE	0.0051	0.0209	0.0493	0.0945	0.1639	0.2714	0.4418	0.7199
	3	WE	0.0051	0.0209	0.0493	0.0945	0.1640	0.2714	0.4417	0.7197
	4	FE	1.0574	1.0979	1.2070	1.3887	1.6668	2.0843	2.7031	3.5842
	4	WE	1.0573	1.0979	1.2069	1.3886	1.6666	2.0839	2.7025	3.5833
	5	FE	0.5189	0.5492	0.6378	0.7904	1.0304	1.3995	1.9599	2.7806
	5	WE	0.5185	0.5489	0.6374	0.7900	1.0299	1.3990	1.9594	2.7802
0.8	1	FE	1.1429	1.1528	1.3077	1.5725	2.0038	2.7131	3.9102	5.9522
	1	WE	1.1428	1.1528	1.3076	1.5723	2.0036	2.7127	3.9097	5.9513
	2	FE	0.0703	0.1392	0.2270	0.3430	0.5093	0.7675	1.1988	1.9568
	2	WE	0.0703	0.1392	0.2270	0.3430	0.5093	0.7674	1.1986	1.9563
	3	FE	0.0054	0.0213	0.0511	0.0997	0.1779	0.3071	0.5318	0.9444
	3	WE	0.0054	0.0213	0.0511	0.0998	0.1779	0.3070	0.5317	0.9441
	4	FE	1.1425	1.1493	1.2950	1.5401	1.9335	2.5720	3.6354	5.4154
	4	WE	1.1424	1.1492	1.2949	1.5399	1.9332	2.5716	3.6347	5.4144
	5	FE	0.5716	0.5880	0.7046	0.9066	1.2388	1.7894	2.7251	4.3272
	5	WE	0.5697	0.5876	0.7042	0.9061	1.2383	1.7890	2.7246	4.3268

Load Case no. 4: Cubic distribution $\sigma(x) = \sigma_0 \left[1 - \left(\frac{x}{r_o - r_i} \right)^3 \right]$ (15d)

Load Case no. 5: periodic distribution $\sigma(x) = \sigma_0 \cos\left(\frac{\pi}{2a}x\right)$ (15e)

The FE simulations are conducted for different ranges and values of the parameters including cylinder geometry α , crack geometry β and, Elastic modulus ratio γ (listed in Table 4).

As it is summarized in Table 4, a total of 1344 runs are carried out in order to obtain unknown coefficients of weight functions.

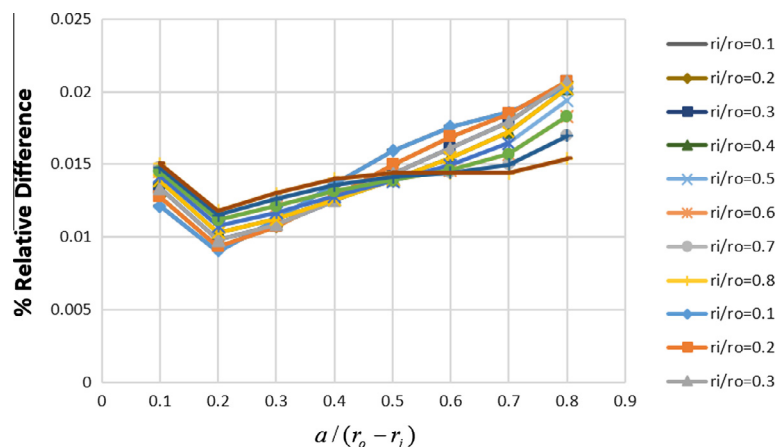


Fig. 6. Relative difference of SIFs between the weight function method and direct FE results for FG cylinders with $\gamma = 0.2$; cubic load case.

Moreover, for the last two load cases, 896 FE runs are carried out, and the SIFs estimated by weight function method are compared with the results calculated directly from these simulations.

In addition, to investigate the accuracy of the weight functions method, the obtained SIFs for FG cylinder with elasticity modulus ratio $\gamma = 10$ under five load cases are compared with the results

extracted from FE analysis and are shown in Table 5. This table also shows that calculated SIFs through weight function method are self-consistent; implying that reference SIFs can be estimated again by the weight function derived from FE simulations.

The percentage of relative difference between the FE and weight function results are defined as follows [17]:

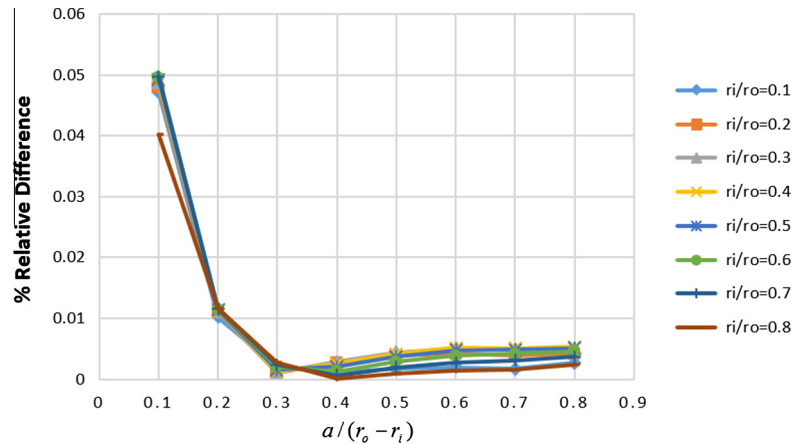


Fig. 7. Relative difference of SIFs between the weight function method and direct FE results for FG cylinders with $\gamma = 0.2$; periodic load case.

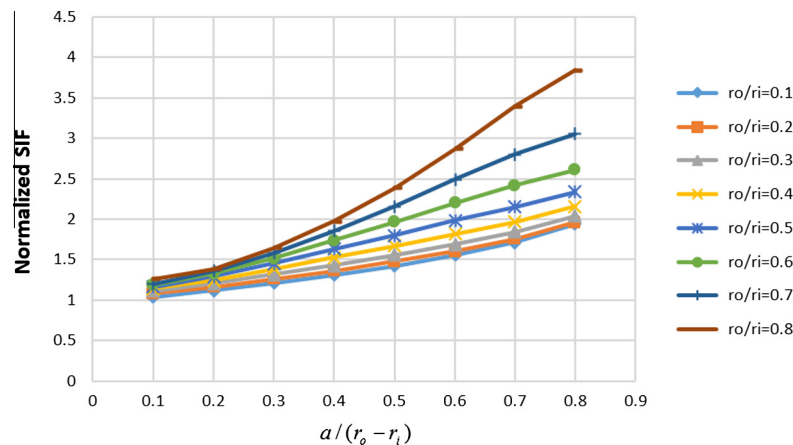


Fig. 8. Normalized SIFs for FG cylinders with $\gamma = 0.5$ predicted by the weight function method; cubic load case.

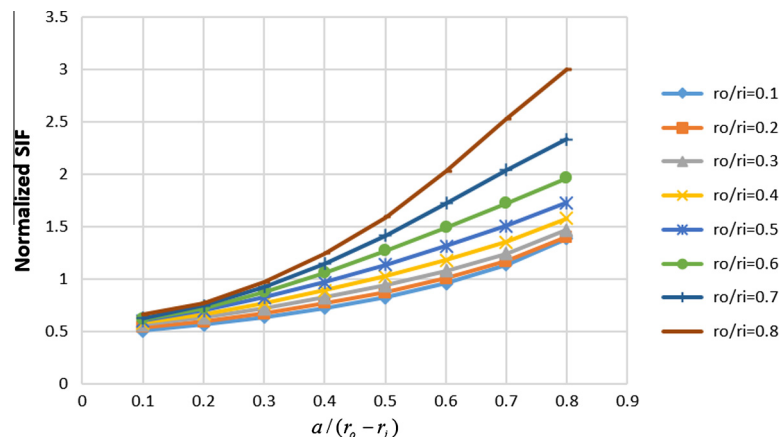


Fig. 9. Normalized SIFs for FG cylinders with $\gamma = 0.5$ predicted by the weight function method; periodic load case.

$$\text{Relative Difference (\%)} = \frac{|K_I^{FE} - K_I^{WF}|}{K_I^{FE}} \times 100 \quad (16)$$

The relative difference for elastic modulus $\gamma = 0.2$ and load cases no. 4 and 5 are presented in Figs. 6 and 7. It is observed that the maximum errors for load case no. 4 (cubic load) and

5 (periodic load) are 0.02% and 0.05%, respectively. Thus, it is found that the weight functions obtained by the first three load cases can predict SIFs for load cases no. 4 and 5 with acceptable accuracy.

SIFs calculated by weight functions for FG cylinder with elasticity modulus ratio $\gamma = 0.5$ under load cases no. 4 (cubic load) and 5 (periodic load) are shown in Figs. 8 and 9. It can be concluded from

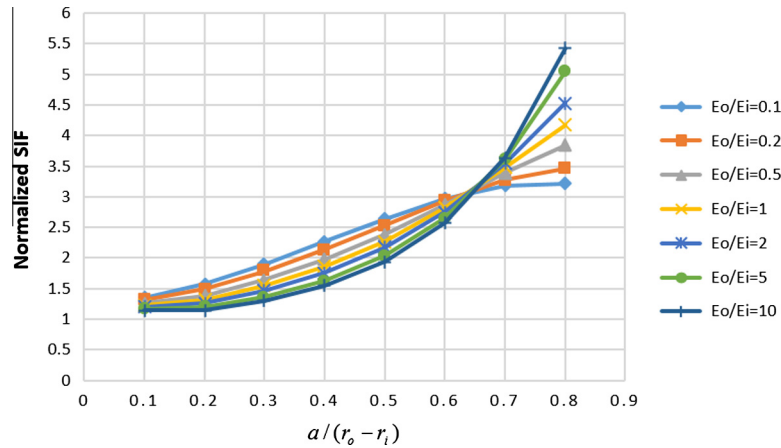


Fig. 10. Normalized SIFs for various elastic moduli ratio with $r_i/r_o = 0.8$ obtained using the weight function method; cubic load case.

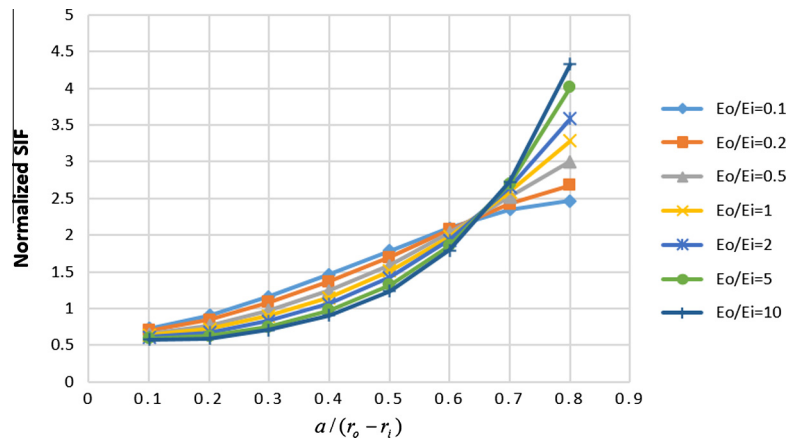


Fig. 11. Normalized SIFs for various elastic moduli ratio with $r_i/r_o = 0.8$ obtained using the weight function method; periodic load case.

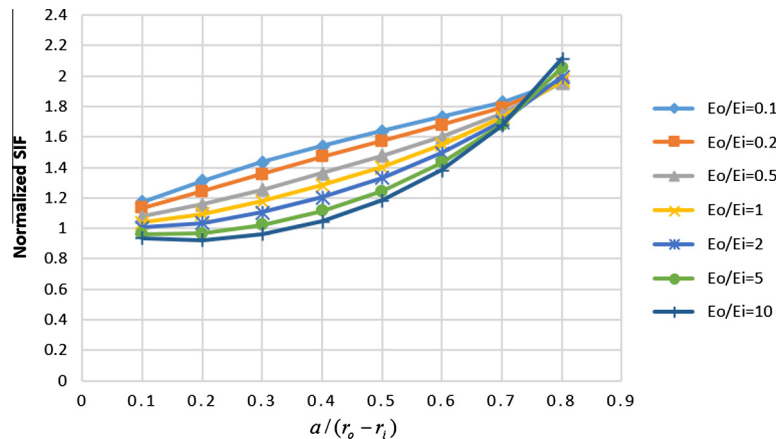


Fig. 12. Normalized SIFs for various elastic moduli ratio with $r_i/r_o = 0.2$ obtained using the weight function method; cubic load case.

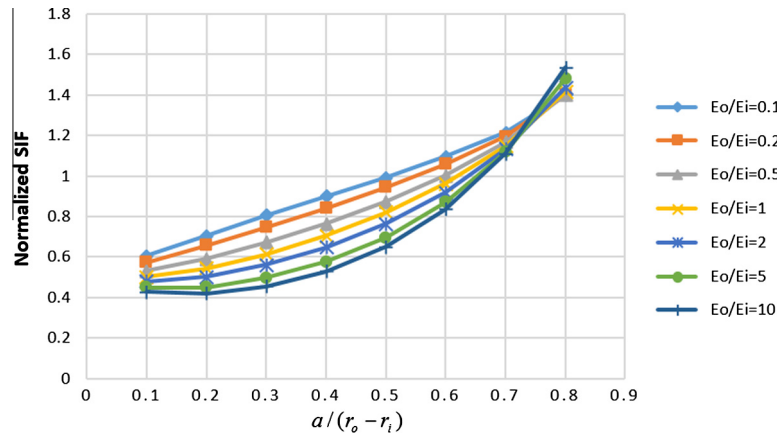


Fig. 13. Normalized SIFs for various elastic moduli ratio with $r_i/r_o = 0.2$ obtained using the weight function method; periodic load case.

these figures that as the crack depth to thickness ratio β increases, SIFs increase more rapidly.

The effects of variations in elastic modulus ratio γ on SIFs under load cases no. 4 (cubic load) and 5 (periodic load), for a cylinder with $\alpha = 0.8$ is presented in Figs. 10 and 11. The remarkable point about these figures is that for $\beta = 0.65$, γ has a negligible effect on SIFs; regardless of the loading condition. Moreover, when $\beta < 0.65$, SIF decreases with an increase in γ . But, with $\beta > 0.65$ as γ increases SIF increases too. The behavior of an FG cylinder with $\alpha = 0.2$ is the same, but the point for which γ has a negligible effect on SIF is at $\beta \approx 0.75$ (shown in Figs. 12 and 13). Predicted SIFs from weight functions are used for plotting these nine diagrams. It can be concluded from these diagrams that for cylinder with two radial cracks as crack depth to thickness ratio increases, SIF also increases.

5. Conclusion

SIFs for mode I of FG cylinders with two internal radial cracks have been obtained using weight function method. Gradient profiles of elastic modulus and Poisson's ratio are considered to be exponential and constant, respectively.

A modified domain form of the energy release rate is used to calculate SIFs from FE analysis in various loading conditions of crack surfaces. In order to determine the unknown coefficients of weight functions, SIFs for three reference load cases are calculated. After the determination of weight function, this method is used to calculate SIFs for two other load cases (cubic and periodic) and the results are compared with the values obtained directly through applying FE analysis, and it is shown that the results from both methods are consistent. Moreover, it is observed that an increase in crack depth to thickness ratio will result in increasing of SIF.

The effect of elasticity modulus ratio on SIF is also investigated. Results show that regardless of the load case on crack surfaces, there is a certain crack depth to thickness ratio at which the effect of gradient profile material on SIF of the cylinder is insignificant. For values of crack depth to thickness ratio lower than this certain point, SIF decreases with an increase in the elasticity modulus. But as the crack depth to thickness ratio passes this point, an increase in elastic modulus ratio will result in increasing of SIF.

References

- [1] A.M. Afsar, M. Anisuzzaman, Stress intensity factors of two diametrically opposed edge cracks in a thick-walled functionally graded material cylinder, *Eng. Fract. Mech.* 74 (2007) 1617–1636, <http://dx.doi.org/10.1016/j.engfracmech.2006.09.001>.
- [2] K. Kurihara, K. Sasaki, M. Kawarada, Adhesion improvement of diamond films, in: *FGM'90-Proceedings of the First International Symposium on Functionally Graded Materials*, 1990, pp. 65–69.
- [3] Y.D. Lee, F. Erdogan, Residual/thermal stresses in FGM and laminated thermal barrier coatings, *Int. J. Fract.* 69 (1994) 145–165.
- [4] F. Erdogan, Fracture mechanics of functionally graded materials, *MRS Bull.* 20 (1995) 43–44.
- [5] J.-H. Kim, G.H. Paulino, Isoparametric graded finite elements for nonhomogeneous isotropic and orthotropic materials, *J. Appl. Mech.* 69 (2002) 502, <http://dx.doi.org/10.1115/1.1467094>.
- [6] J.-H. Kim, G.H. Paulino, Finite element evaluation of mixed mode stress intensity factors in functionally graded materials, *Int. J. Numer. Methods Eng.* 53 (2002) 1903–1935, <http://dx.doi.org/10.1002/nme.364>.
- [7] Y. Wei, C.F. Shih, Fracture along an interlayer, *Int. J. Solids Struct.* 31 (1994) 985–1002, [http://dx.doi.org/10.1016/0020-7683\(94\)90007-8](http://dx.doi.org/10.1016/0020-7683(94)90007-8).
- [8] Z.-H. Jin, R.C. Batra, Some basic fracture mechanics concepts in functionally graded materials, *J. Mech. Phys. Solids* 44 (1996) 1221–1235.
- [9] M.C. Walters, G.H. Paulino, R.H. Dodds, Stress-intensity factors for surface cracks in functionally graded materials under mode-I thermomechanical loading, *Int. J. Solids Struct.* 41 (2004) 1081–1118, <http://dx.doi.org/10.1016/j.ijsolstr.2003.09.050>.
- [10] B. Yildirim, S. Dag, F. Erdogan, Three dimensional fracture analysis of FGM coatings under thermomechanical loading, *Int. J. Fract.* 132 (2005) 371–397, <http://dx.doi.org/10.4028/www.scientific.net/MSF.492-493.373>.
- [11] C. Zhang, M. Cui, J. Wang, X.W. Gao, J. Sladek, V. Sladek, 3D crack analysis in functionally graded materials, *Eng. Fract. Mech.* 78 (2011) 585–604, <http://dx.doi.org/10.1016/j.engfracmech.2010.05.017>.
- [12] H.F. Bueckner, Novel principle for the computation of stress intensity factors, *Z. Fuer Angew. Math. Mech.* 50 (1970).
- [13] J.R. Rice, Some remarks on elastic crack-tip stress fields, *Int. J. Solids Struct.* 8 (1972) 751–758, [http://dx.doi.org/10.1016/0020-7683\(72\)90040-6](http://dx.doi.org/10.1016/0020-7683(72)90040-6).
- [14] T.L. Anderson, T.L. Anderson, *Fracture Mechanics: Fundamentals and Applications*, CRC Press, 2005.
- [15] T. Fett, D. Munz, A weight function for cracks in gradient materials, *Int. J. Fract.* 84 (1997) L3–L7.
- [16] T. Fett, D. Munz, Y.Y. Yang, Direct adjustment procedure for weight functions of graded materials, *Fatigue Fract. Eng. Mater. Struct.* 23 (2000) 191–198.
- [17] I. Eshraghi, N. Soltani, Stress intensity factor calculation for internal circumferential cracks in functionally graded cylinders using the weight function approach, *Eng. Fract. Mech.* 134 (2015) 1–19, <http://dx.doi.org/10.1016/j.engfracmech.2014.12.007>.
- [18] I. Eshraghi, N. Soltani, Thermal stress intensity factor expressions for functionally graded cylinders with internal circumferential cracks using the weight function method, *Theor. Appl. Fract. Mech.* 80 (2015) 170–181, <http://dx.doi.org/10.1016/j.tafmec.2015.09.003>.
- [19] M. Shi, H. Wu, L. Li, G. Chai, Calculation of stress intensity factors for functionally graded materials by using the weight functions derived by the virtual crack extension technique, *Int. J. Mech. Mater. Des.* 10 (2014) 65–77, <http://dx.doi.org/10.1007/s10999-013-9231-0>.
- [20] H. Wu, L. Li, G. Chai, F. Song, T. Kitamura, Three-dimensional thermal weight function method for the interface crack problems in bimaterial structures under a transient thermal loading, *J. Therm. Stress.* 39 (2016) 371–385, <http://dx.doi.org/10.1080/01495739.2016.1152108>.
- [21] I.S. Raju, J.C. Newman, Stress-intensity factors for internal and external surface cracks in cylindrical vessels, *J. Press. Vessel Technol.* 104 (1982) 293, <http://dx.doi.org/10.1115/1.3264220>.
- [22] C.P. Andrasic, A.P. Parker, D. Stress, I. Factors, Dimensionless stress intensity factors for cracked thick cylinders under polynomial crack face loadings, *Eng. Fract. Mech.* 19 (1984) 187–193.
- [23] B.S. Institution, Guide to the Methods for Assessing the Acceptability of Flaws in Metallic Structures, British Standard Institution, 1999.

- [24] G. Glinka, G. Shen, Universal features of weight functions for cracks in mode I, Eng. Fract. Mech. 40 (1991) 1135–1146, [http://dx.doi.org/10.1016/0013-7944\(91\)90177-3](http://dx.doi.org/10.1016/0013-7944(91)90177-3).
- [25] H. Petroski, J. Achenbach, Computation of the weight function from a stress intensity factor, Eng. Fract. Mech. 10 (1978) 257–266, [http://dx.doi.org/10.1016/0013-7944\(78\)90009-7](http://dx.doi.org/10.1016/0013-7944(78)90009-7).
- [26] T. Fett, D. Determination, O.F.W. Functions, F. Reference, L. Cases, Direct determination of weight functions from reference loading cases and geometrical conditions, Eng. Fract. Mech. 42 (1992) 435–444.
- [27] T. Fett, D. Munz, Y.Y. Yang, Applicability of the extended Petroski-Achenbach weight function procedure to graded materials, Eng. Fract. Mech. 65 (2000) 393–403. <<http://www.scopus.com/inward/record.url?eid=2-s2.0-0034149067&partnerID=tZOTx3y1>>.
- [28] S. Dag, Thermal fracture analysis of orthotropic functionally graded materials using an equivalent domain integral approach, Eng. Fract. Mech. 73 (2006) 2802–2828, <http://dx.doi.org/10.1016/j.engfracmech.2006.04.015>.
- [29] S.G. Flncv, U.S. Fish, W. Service, L.F. Pnnx, E.T. Road, F. Delale, F. Erdogan, The crack problem for a nonhomogeneous plane, J. Appl. Mech. 50 (1983) 609–614.
- [30] F. Erdogan, B.H. Wu, The surface crack problem for a plate with functionally graded properties, J. Appl. Mech. 64 (1997) 449–456.
- [31] J. Kim, G.H. Paulino, Mixed-mode fracture of orthotropic functionally graded materials using finite elements and the modified crack closure method, Eng. Fract. Mech. 69 (2002) 1557–1586, [http://dx.doi.org/10.1016/S0013-7944\(02\)00057-7](http://dx.doi.org/10.1016/S0013-7944(02)00057-7).
- [32] ABAQUS Documentation and User Manual, Version 6.12, Simulia, Dassault Systèmes, 2012.